Protein & Science

Localization of binding sites in protein structures by optimization of a composite scoring function

Andrea Rossi, Marc A. Marti-Renom and Andrej Sali

P<P	Published online September 8, 2006 in advance of the print journal.
Email alerting service	Receive free email alerts when new articles cite this article - sign up in the box at the top right corner of the article or **click here**

Notes

Advance online articles have been peer reviewed and accepted for publication but have not yet appeared in the paper journal (edited, typeset versions may be posted when available prior to final publication). Advance online articles are citable and establish publication priority; they are indexed by PubMed from initial publication. Citations to Advance online articles must include the digital object identifier (DOIs) and date of initial publication.

To subscribe to _Protein Science_ go to:
http://www.proteinscience.org/subscriptions/

Localization of binding sites in protein structures by optimization of a composite scoring function

ANDREA ROSSI, MARC A. MARTI-RENOM, AND ANDREJ SALI

Departments of Biopharmaceutical Sciences and Pharmaceutical Chemistry, California Institute for Quantitative
Biomedical Research, University of California, San Francisco, California 94143-2552, USA

Abstract

The rise in the number of functionally uncharacterized protein structures is increasing the demand
for structure-based methods for functional annotation. Here, we describe a method for predicting the
location of a binding site of a given type on a target protein structure. The method begins by
constructing a scoring function, followed by a Monte Carlo optimization, to find a good scoring patch on
the protein surface. The scoring function is a weighted linear combination of the z-scores of various
properties of protein structure and sequence, including amino acid residue conservation, compactness,
protrusion, convexity, rigidity, hydrophobicity, and charge density; the weights are calculated from a set
of previously identified instances of the binding-site type on known protein structures. The scoring
function can easily incorporate different types of information useful in localization, thus increasing the
applicability and accuracy of the approach. To test the method, 1008 known protein structures were split
into 20 different groups according to the type of the bound ligand. For nonsugar ligands, such as various
nucleotides, binding sites were correctly identified in 55%–73% of the cases. The method is completely
automated (http://salilab.org/patcher) and can be applied on a large scale in a structural genomics
setting.

Keywords: protein function annotation; small ligand binding-site localization

Many protein targets of structural biologists are no longer chosen because of their function, but rather by their location in the protein sequence-structure space (Burley et al. 1999; Brenner 2000, 2001; Sali 2001; Vitkup et al. 2001; Chance et al. 2002; Goldsmith-Fischman and Honig 2003). Therefore, the number of functionally uncharacterized protein structures is growing. Of the 36,606 entries in the Protein Data Bank (PDB) (Kouranov et al. 2006) as of February 23, 2006, 1407 structures were deposited by structural genomics consortia, 985 (70%) of which had an unknown function according to the HEADER record of their PDB files. In contrast, only 174 (0.5%) of the 35,199 protein structures solved outside of structural genomics had no functional annotations in their PDB files.

To classify the functions of thousands of uncharacterized protein structures that will become available over the next few years and millions of comparative models based on the known structures, automated structure-based functional annotation is required (Wallace et al. 1996, 1997; Kleywegt 1999; Thornton et al. 2000; Babbitt 2003; Laskowski et al. 2003). In particular, we need to be able to identify the locations and types of binding sites on a given structure, because the binding sites define the molecular function of a protein.

The most principled computational approach to predicting the molecular function is to dock a large library of potential ligands against the surface of the protein. In

practice, because of the inaccuracies of the available scoring functions and difficulties in the conformational and configurational sampling, few such attempts have been made (Greenbaum et al. 2002; Macchiarulo et al. 2004). Furthermore, most docking programs require a specification of the location of the binding site as part of their input. Thus, the first step in ligand docking is usually to localize the likely binding site on the surface of the target protein. The binding sites are generally cavities on protein surfaces, often the largest ones (Kuntz et al. 1982; Laskowski et al. 1996; Liang et al. 1998; Brady and Stouten 2000). However, not all cavities on the surface of a protein are binding sites, and it is not well understood what distinguishes binding sites from other cavities (Ringe 1995). Mapping the surface of the protein with molecular probes, such as organic solvent molecules, and calculating energetically favorable locations for ligands helps to detect binding sites on the surface of a protein structure (Goodford 1985; Miranker and Karplus 1991; Silberstein et al. 2003). Other methods identify hot spots, defined as destabilizing residues on the surface of a protein that may therefore be part of a binding site (Elcock 2001).

One of the simplest bioinformatics approaches to localizing binding sites depends on the availability of a set of related sequences. The binding site is predicted to correspond to a set of contiguous surface residues that are also evolutionarily conserved in the corresponding multiple sequence alignment (Zvelebil et al. 1987; Mirny and Shakhnovich 1999; del Sol Mesa et al. 2003). This strategy works to some degree because evolution tends to conserve functionally important residues. Another approach uses a principal components analysis to find a set of spatially local positions in a multiple sequence alignment whose clustering mimics the known functional classification of the group (Casari et al. 1995). A related approach, the evolutionary trace method, also exploits the conservation of function within a family and variation of function between families of a superfamily (Lichtarge et al. 1996; Aloy et al. 2001; Armon et al. 2001; Landgraf et al. 2001; Madabushi et al. 2002; del Sol Mesa et al. 2003; Yao et al. 2003), benefiting from a multiple sequence alignment, the corresponding phylogenetic tree, and the three-dimensional structure of at least one member of the superfamily. The conservation-based and evolutionary trace methods appear to have similar accuracies (del Sol Mesa et al. 2003), although a rigorous assessment is difficult because of its dependence on the testing data set and the testing criteria.

The conservation-based and evolutionary trace methods listed above can be applied even when binding-site locations are unknown for all homologs in the set. In contrast, homology-based approaches use information about related protein sequences and structures with known binding-site locations. Detection of sequence similarity between an uncharacterized target and a characterized template has been the most frequently used method to identify the locations of functional sites (Bork et al. 1998). However, these methods become less accurate as the evolutionary distance between the two proteins increases (Eisenstein et al. 2000; Moult and Melamud 2000; DeWeese-Scott and Moult 2004). In addition, while the functional binding sites can be detected by looking at the sequence conservation, many drugs interfere with the protein function by binding at the secondary binding sites (Hardy and Wells 2004).

At the sequence level, local sequence patterns have been successfully applied to function prediction even in the absence of high-sequence similarity (Bairoch and Bucher 1994). At the structure level, 3D-motifs (i.e., conserved spatial arrangements of side chains, residues, and/or secondary structure segments) have also been successfully used to identify binding sites of the same type in proteins with different folds (Artymiuk et al. 1994; Wallace et al. 1996, 1997; Kleywegt 1999; Oldfield 2002; Stark and Russell 2003; Stark et al. 2003). Another related approach to comparing binding sites relies on five different chemical descriptors that describe the cavity of a protein, thus allowing a comparison of binding sites independently from sequence and structure similarities (Schmitt et al. 2002). Several other approaches that use invariant physical properties of the binding site were also described for characterization of protein–ligand, protein–protein, and protein–DNA interactions (Rosen et al. 1998; Pawlowski and Godzik 2001; Chakrabarti and Janin 2002; Kinoshita and Nakamura 2003; Ahmad et al. 2004; Neuvirth et al. 2004; Deremble and Lavery 2005).

While the existing methods provide useful ways to identify and describe binding sites, the problem of accurate identification of the location of a binding site of a given type on a target protein structure is not solved. We suggest that a method capable of integrating a variety of different types of information about the given protein structure, its binding site, and its homologs is likely to do better than any one of the methods based on a subset of information. We describe here such a method. The integration is expressed as an optimization problem that depends on a representation of protein-binding sites, a composite scoring function for evaluating the likelihood that any patch of residues is a binding site of the required type, and a sampling protocol that searches for good scoring patches (Fig. 1; see Methods).

Below, we describe the localization method and the benchmarking criteria (Methods). Then, we assess the accuracy of the method and illustrate it by several sample applications (Results). We conclude by discussing the implications of the approach for automated functional annotation of proteins (Discussion).
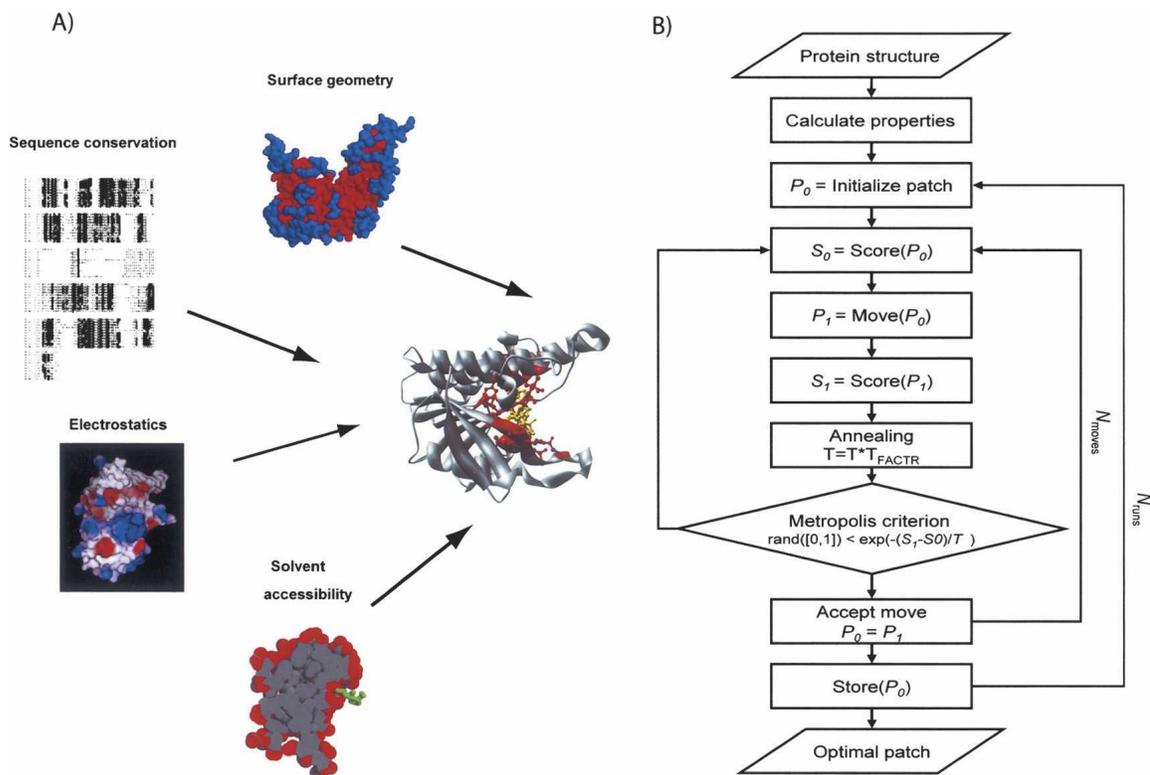
Figure 1. (*A*) Scheme of the integration of different properties into a single scoring function to localize the binding site of a given type in a target protein structure (see Methods). (*B*) Flowchart of the optimization protocol (see Methods).

Methods

We aim to maximize the accuracy of the localization of a binding site of known type on a target protein structure by combining varied information about the binding site (Fig. 1A). This aim is achieved by expressing the problem as an optimization problem, which requires a representation of the protein and its binding site, a scoring function, and an optimization algorithm. We describe the three aspects of the approach next.

Binding-site representation and patch definition

The binding site is predicted by identifying the patch with the optimal score. A patch consists of a set of contiguous surface residues. By definition, a surface residue must have at least one atom with accessible solvent area (ASA) larger than 2 Å^2. A residue that is not on the surface is a core residue. Two surface residues are contiguous if the closest exposed atoms from the two residues are <6 Å apart.

Composite scoring function

The scoring function is a weighted combination of seven properties. These properties were chosen to represent a variety of features of binding sites that generally distinguish them from the rest of the protein, such as their evolution (sequence conservation), shape (compactness, protrusion, and convexity), energetics (hydrophobicity and charge density), and dynamics (rigidity).

Sequence conservation

The first property is based on the observation that most binding sites are likely to be relatively conserved in sequence because of the evolutionary pressure to keep the binding sites intact (Introduction). Sequence conservation of a given patch is defined as the average Shannon entropy (Shannon 1948) of the residues in the patch. The Shannon entropy at a given multiple sequence alignment position is

$$C_i = \sum_{j=1..20} p_j(i) \log p_j(i)$$

where $p_j(i)$ is the frequency of residue j at position i based on a multiple sequence alignment generated by the program PSI-BLAST, with default parameters except for the e-value threshold of 10^{-5}. The search database is Uniprot with ~3.2 million sequences (Wu et al. 2006); the query sequence is the target protein whose binding site is being localized.

Compactness

To encode the shape of the patch, compactness is defined as the average distance between the residues that form a patch:

$$f_{comp}(P) = \frac{1}{N_d} \sum_{i,j \in P} d_{ij}$$

where N_d is a normalization factor corresponding to the number of considered distances (i.e., $N_d = \sum_{i,j \in P} 1$) and d_{ij} is the distance between the two closest surface atoms of residues i and j in the patch P.

Protrusion

Patch protrusion is defined as the percentage of protruding residues in the patch (Fig. 2A). A residue is protruding if at least 50% of its atoms are protruding. An atom is protruding if the number of neighboring atoms (i.e., the number of atoms that lie between 8 and 12 Å from the query atom) is <120. These two parameters were determined by visual inspection of protein structures.

Convexity

Another geometrical property, patch convexity, is determined by averaging the residue convexity for each residue in the patch (Fig. 2B). The convexity of residue i is obtained by considering N_i nearest-neighbor residue pairs involving residue i (*n.n.res.*):

$$f_{conv}(i) = \frac{1}{N_i} \sum_{j \in n.n.res.} \left(\frac{d_{ij}^{solv}}{d_{ij}^{exp}} - 1 \right)$$

where d_{ij}^{solv} and d_{ij}^{exp} are the distances between the "solvent points" and "exposed centroids" of residues i and j, respectively (Fig. 2B).

Rigidity

Flexibility of the native structure is likely to have a role in many protein–ligand interactions. The rigidity of a patch is calculated as the average B-factor of the exposed atoms involved in the patch. All B-factors are obtained from the crystallographic PDB files. A measure of flexibility determined by NMR spectroscopy could also be used.

Hydrophobicity

The hydrophobic effect frequently plays an important role in protein–ligand recognition. The hydrophobicity of a patch is calculated as the average hydrophobicity of the residues in the patch. The residue hydrophobicity is obtained from the experimentally derived scale of Fauchere (Fauchere and Pliska 1983).

Charge density

Atomic charges are many times responsible for the specificity of protein–ligand recognition. Charge density of a patch is the sum of charges for its exposed atoms divided by the solvent accessibility area of the patch. Atomic charges are obtained from the CHARMM22 force field (MacKerell et al. 1998).

Scoring function 1: Linear model

The linear scoring function favors binding-site predictions that maximize the difference observed between random patches and known examples of a given
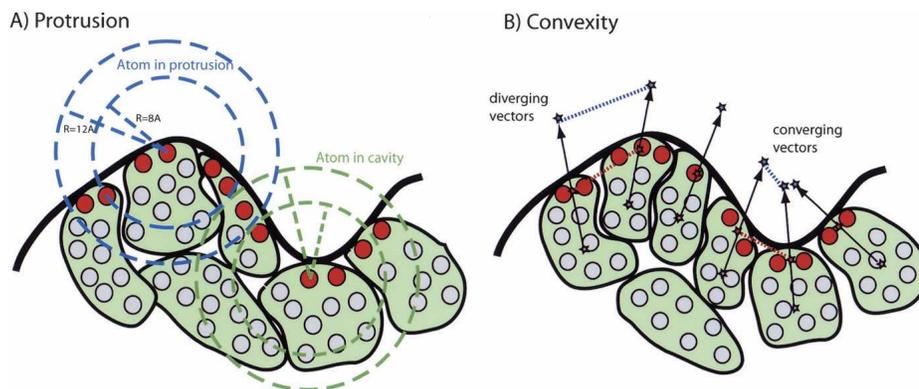

Figure 2. Schematic representations of protrusion and convexity (see Methods). (*A*) Protrusion is calculated by counting the number of neighboring atoms. The atom count is very different for a protruding atom and an atom in a cavity. (*B*) Convexity is determined by using three different types of reference points. For every exposed residue, the exposed and buried centroids (represented by the red and the gray stars) are the geometrical centers of the exposed and buried atoms, respectively. The "solvent point" (blue star) is located on the exposed side of a line connecting the buried and exposed centroids 3 Å away from the exposed centroid.

binding-site type. First, each one of the seven properties defined above is normalized by transforming its value f into a z-score $\tilde{f} = (f - \langle f \rangle)/\sigma_f$. Both the average $\langle f \rangle$ and the standard deviation σ_f are obtained from a sample of 1000 random patches, generated as described below. The normalization of the seven properties is useful because it puts them all on the common scale for subsequent comparisons.

Second, the seven z-scores are summed

$$F(P) = \sum_{k=1}^{7} w_k \cdot \tilde{f}_k(P),$$

where k denotes the property type and P is a patch. The weights w_k determine the relative importance of each property in the search for the binding-site location. Both the absolute values $|w_k|$ and the signs of the weights sign w_k are crucial; the relative magnitude controls the importance that each single property has in the scoring function, while the sign controls whether the property is maximized or minimized.

This scoring function can be used for different types of binding sites by adjusting the property weights. Here, we calculate the weights independently for each type of the binding site from a sample of structurally defined binding sites of the required type. The weight of each property is calculated as the average of the z-scores obtained from a training set of known binding sites $\{P_i\}$ of the given type:

$$w_k = \frac{1}{M} \sum_{i=1}^{M} \tilde{f}_k(P_i)$$

where M is the number of binding sites in the training set. Therefore, properties that have consistently positive (negative) z-scores will be positively (negatively) weighted and properties with z-scores fluctuating around zero will have small weights. Each binding-site type is described quantitatively by the seven property weights w_k, forming a fingerprint of the binding site. Unless otherwise noted, we use scoring function 1 in this work.

Scoring function 2: Quadratic model

The quadratic scoring function favors binding-site predictions that are similar to known examples of a given binding-site type:

$$F(P) = \sum_{k=1}^{7} w_k \cdot \left(\frac{f_k(P) - \lambda_k}{\sigma_k} \right)^2$$

where λ_k and σ_k are the average and standard deviation of property k for the known binding sites (positives), respectively. The weight of property k depends on the

dissimilarity between the distributions of the property for the known binding sites and random patches as quantified by the Fisher's discriminant ratio (Theodoridis and Koutroumbas 1999):

$$w_k = \frac{(\lambda_k - \lambda'_k)^2}{\sigma_k^2 + \sigma_k'^2},$$

where λ'_k and σ'_k are the average and standard deviation for the random patches (negatives), respectively.

Patch optimization

To find the optimal patch corresponding to the maximum of the scoring function, we need to explore the space of all possible patches. Unfortunately, given the limitations of computer power, this problem generally cannot be solved by an exhaustive enumeration of all patches. Thus, we used stochastic Monte Carlo Simulated Annealing (MCSA) optimization (Fig. 1B; Kirkpatrick et al. 1983).

The first step in the MCSA optimization algorithm is the generation of an initial random patch. First, a surface residue is randomly selected to be the seed residue of a patch. Next, other contiguous residues are sequentially added to the patch until the patch consists of a predefined number of residues. The number of residues in a given patch is a random number from a uniform distribution defined by a set of known binding sites of the required type; in particular, the average and range of the uniform distribution were set to the average and twice the standard deviation of the binding-site size for the sample.

Next, the initial random patch is modified iteratively, by repetitive application of a move that involves a random addition and deletion of a residue from the patch. Only moves that do not destroy the contiguity of the patch are considered. The difference in the scores after and before the move, $\Delta F(P)$, is recorded. The move is accepted according to the standard Metropolis criterion with the following probability (Metropolis et al. 1953):

$$P(T) = \begin{cases} 1 & \text{if } \Delta F(P) < 0 \\ \exp(-\Delta F(P)/T) & \text{otherwise} \end{cases}$$

The Monte Carlo temperature T plays a major role in the MCSA. At high values of T, most moves are accepted, without strongly discriminating between uphill and downhill moves. At low T, primarily moves that decrease the score are accepted. The initial temperature was set to 1 and decreased at each minimization step by a factor of 0.999. Each optimization consisted of 10,000 such iterations. For each binding-site localization, 100 optimizations are performed, starting each time with a different, randomly selected seed residue.

Testing binding-site localization

Testing sets of binding sites

We relied on the LIGBASE database (November 2003) (Stuart et al. 2002) to extract a list of binding sites from protein structures deposited in the PDB. A binding site is defined as all of the protein residues with at least one atom within 5Å of any of the ligand atoms. We restrict the data set to 20 different ligands of 10 or more heavy atoms that occur >100 times in LIGBASE. The set contains biologically relevant molecules (such as ATP, NAD, and sugars), but excludes ions and very small molecules. To avoid redundancy, we filtered the sample proteins so that all pairs of accepted structures satisfied the following three conditions: (1) The fraction of the $C\alpha$ atoms that superpose within 4 Å is <90%, (2) the corresponding $C\alpha$ RMSD is larger than 2 Å, and (3) sequence identity is <30%; alignments in DBAli (Marti-Renom et al. 2001) were used for this filtering. Finally, when more than one ligand interacted with a single chain, only one binding site was selected randomly (Table 1).

Testing protocol

To test the method, we used the jackknife protocol in which the structure whose binding site was localized was not used in the calculation of the scoring function parameters.

Accuracy of predictions

The accuracy of the localization prediction is assessed by an overlap between the actual and predicted binding sites. Given two patches, P_1 and P_2, with a number of residues, N_1 and N_2, respectively, the overlap between them is

$$\vartheta(P_1, P_2) = \frac{N_1 \cap N_2}{\min(N_1, N_2)}$$

where $N_1 \cap N_2$ is the number of overlapping residues and $\min(N_1, N_2)$ is their minimum value. The overlap of two patches is 1 if they are identical or one patch is completely contained within the other. The overlap is 0 if there are no residues in the intersection between the two.

For each test set, the overall accuracy of predictions is defined as the fraction of binding sites correctly localized. A binding site is considered correctly localized if the overlap ϑ of the best scoring patch with the actual binding site is greater than a predefined cutoff ϑ_0. Unless otherwise specified, we use $\vartheta_0 = 0.5$.

Accuracy of random patches as a control

The difficulty of localization correlates with a variety of attributes, such as the average sizes of the protein, binding site, and the optimized patch. Some ligands may

Table 1. *List of the 20 ligand types used in the testing of binding site localization*

Three-letter code	Extended name	Type	All instances[a]	Nonredundant instances[b]
ADP	Adenosine disphosphate	Nucleotide	552	129
AMP	Adenosine monophosphate	Nucleotide	185	29
ANP	Phosphoaminophosphonic acid-adenilate ester	Nucleotide	167	41
ATP	Adenosine trisphosphate	Nucleotide	294	53
BOG	B-octylglucoside	Glucoside	217	24
CIT	Citric acid	Acid	211	33
FAD	Flavin-adenine dinucleotide	Nucleotide	540	64
FMN	Flavin mononucleotide	Nucleotide	279	40
FUC	Fucose	Sugar	304	20
GAL	D-galactose	Sugar	541	38
GDP	Guanosine diphosphate	Sugar	179	22
GLC	Glucose	Sugar	1097	58
HEC	Heme C	Protophorphyrin	199	19
HEM	Heme	Protophorphyrin	2093	129
MAN	Alpha D-mannose	Sugar	1438	33
MES	Ethanesulphonic acid	Solvent	187	36
NAD	Nicotinamide adenine dinucleotide	Nucleotide	742	104
NAG	N-acetylglucosamine	Glucosamine	1950	81
NAP	Nicotinamide adenine dinucleotide phosphate (NADP)	Nucleotide	258	29
NDP	Dihydro-nicotinamide adenine dinucleotide phosphate	Nucleotide	208	26

[a] Number of instances in PDB (Kouranov et al. 2006) according to LIGBASE (Stuart et al. 2002).
[b] Number of instances after removing chain redundancy.

bind prevalently to large multidomain proteins, where the localization of the binding site is statistically more difficult because there are more nonbinding than binding residues compared with smaller proteins. For this reason, we compare the accuracy of localization relative to the accuracy obtained by randomly selecting a surface patch. The random patches correspond to the starting patches for the MCSA optimization.

Results

We now validate our optimization algorithm with an ideal scoring function and then we optimize the scoring function weights for all of the binding-site types considered in this paper (Table 1). Finally, after describing a sample binding-site localization, we assess the performance of our method with the aid of the whole testing data set.

Testing the optimization algorithm

It is necessary, although not sufficient, that a good optimizer finds a substantially correct solution when an ideal scoring function is used. We tested our MCSA sampling protocol with a scoring function that corresponds to the native overlap between a scored patch and the actual binding site. Otherwise, the default values of various parameters, such as the initial temperature and the temperature-scaling factor, were used (see Methods). For a small number of arbitrarily chosen test cases, the known global minimum is almost always reached in 3000–4000 MC steps (Fig. 3). Moreover, even for realistic scoring
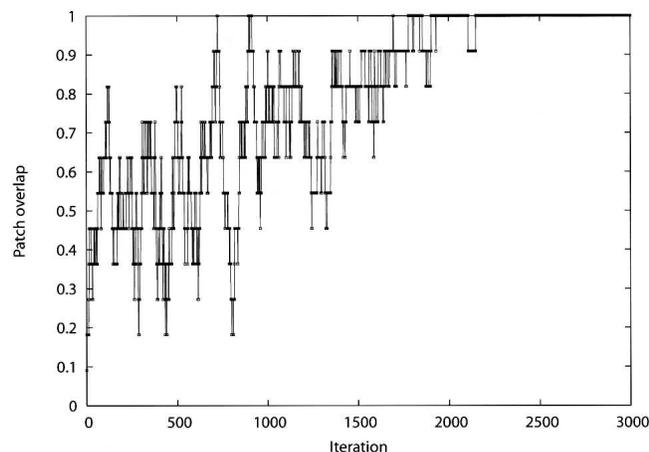

Figure 3. Patch overlap as a function of the iteration number during a simulated annealing optimization. To test the efficiency of the MCSA protocol, the scoring function was replaced with the patch overlap. Under these ideal conditions, the program always retrieves the correct solution. The test involves predicting the location of the NAD binding site on dihydropteridine reductase (PDB ID 1dhr).

functions, the algorithm tends to produce the same best-scoring solution for different, randomly selected starting patches. Therefore, we conclude that the optimizer is not likely to limit the accuracy of our predictions.

Property distributions and fingerprints

As described in Methods, the scoring function is either a linear combination of individual property scores (linear model) or a linear combination of terms quadratic in the property scores (quadratic model). The weights and the other parameters are calculated from the distribution of the properties of the known binding sites and random patches. While random patches do not depend on the type of ligand, the distribution for known binding sites is specific to the binding-site type.

As an example, we describe the distribution of the NAD binding-site properties (Fig. 4). The z-scores of sequence conservation, hydrophobicity, protrusion, and convexity are consistently negative or positive for most of the protein–NAD complexes in our training data set. Accordingly, these properties will be important in discriminating a binding site from a random patch and should contribute to the scoring function more than the properties that are similar between the actual binding sites and random patches. The less discriminating properties include the compactness, charge density, and rigidity. The average of their z-scores is close to 0, varying from positive to negative values for the different known protein–NAD complexes.

We determined the property weights for all 20 binding-site types considered in this paper (Table 1; see Methods). For some properties, the seven z-scores are consistently positive or negative, while others change sign for different ligands. For example, rigidity of all binding-site types is consistently higher than that of a random surface patch, while the sequence is usually more conserved, although it can also be slightly more variable for ligands such as fucose and mannose. This difference in the distributions is reflected in the weights and, in the case of the quadratic model, in the other parameters of the scoring function. The set of parameters determined from a given training set of binding sites is specific to the corresponding ligand type and constitutes the fingerprint of the ligand (Table 2).

Fingerprints and ligand similarity

In general, similar ligands should bind to similar binding sites and should therefore have similar fingerprints. We explored whether this is actually the case by clustering the fingerprints. We calculated a dendrogram of fingerprints, based on the Euclidean distances between pairs of fingerprints (Fig. 5). Similar ligands indeed tend to cluster together. For example, ligands containing the adenine
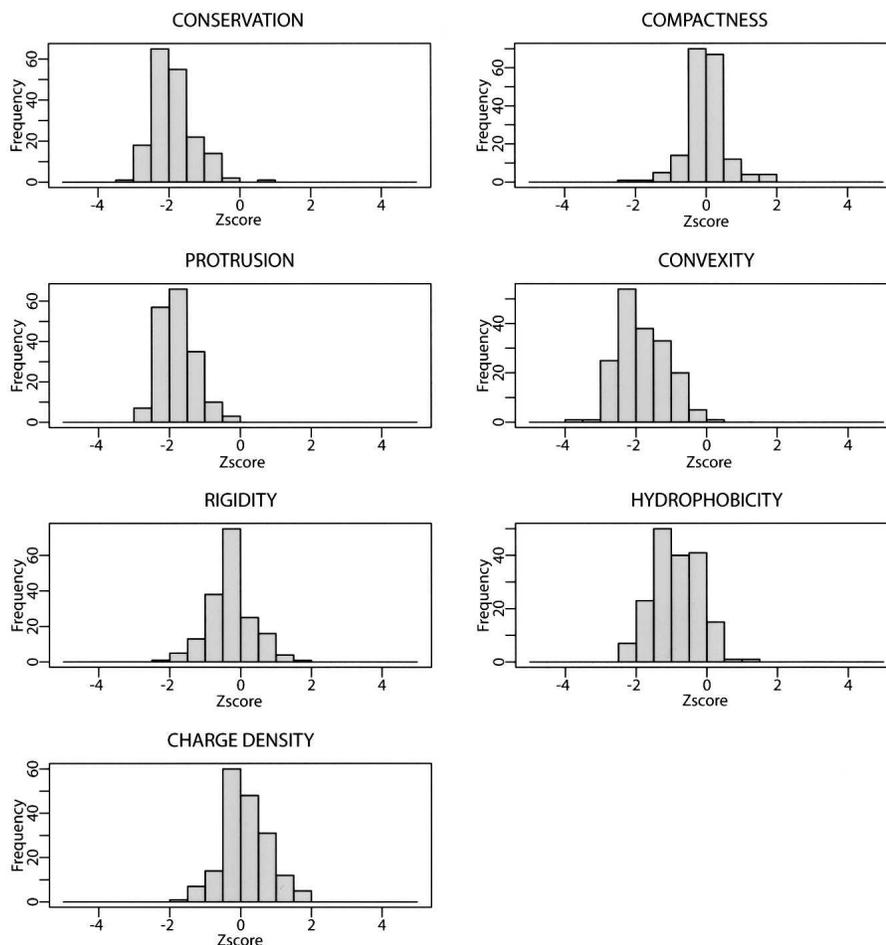
Figure 4. Distributions of the NAD binding-site properties. All the properties have a unimodal distribution. Properties having their peak around zero (i.e., compactness, protrusion, rigidity, and charge density) are less informative than those with their peak far from zero (i.e., conservation, hydrophobicity, and convexity).

moiety, such as ADP, ANP, and ATP, cluster in the lower arm of the tree, while sugars such as fucose, mannose, and glucose cluster in the upper arm. This clustering of the ligands by their fingerprints demonstrates that the fingerprints capture characteristics of the ligands, even though these characteristics were not used in the fingerprint construction.

An example: Dihydropteridine reductase

We illustrate our method for binding-site localization by its application to the dihydropteridine reductase enzyme (DHPR) that binds the NAD cofactor. NAD binding-site position was determined by comparison with the corresponding native structure of the protein–ligand complex extracted from the PDB (code 1dhr) ((Fig. 6A; Varughese et al. 1992). The ability of our method to localize the NAD binding site was assessed by comparing the overlap between the binding site and 100 independently optimized patches with the overlap between the binding site and 100 random surface patches (see Methods).

The best-scoring binding-site prediction overlaps with the actual binding site for 10 of 11 residues (Fig. 6B). Of the 100 independently predicted binding sites, ~50% have an overlap larger than 0.8 and only ~20% have an overlap below 0.5 (Fig. 6C). In contrast, for random surface patches, 97% have an overlap of ≤0.4 and 47% of the patches have no overlap at all. These results clearly indicate that the predicted binding sites are much closer to the actual binding site than the randomly generated surface patches. Moreover, the correlation between the binding-site overlap and the score is higher for the binding-site predictions (0.74) than for the random surface patches (0.47) (Fig. 6D). In summary, for this particular example, the scoring function is sufficiently accurate and the optimizer sufficiently thorough for correct binding-site localization.

Table 2. *Binding-site fingerprints for the 20 ligands*

Ligand	Conservation	Compactness	Protrusion	Convexity	Rigidity	Hydrophobicity	Charge density
ADP	−1.87	−1.51	−1.46	−1.37	−0.36	−0.08	0.35
AMP	−2.08	−1.99	−1.99	−1.99	−0.42	−0.48	0.35
ANP	−1.96	−1.21	−1.67	−1.71	−0.26	−0.10	0.14
ATP	−2.12	−1.32	−1.73	−1.68	−0.28	0.09	0.21
BOG	−0.14	−2.03	−0.41	−0.61	−0.45	−1.07	0.70
CIT	−1.40	−3.02	−1.09	−1.09	−0.47	−0.09	0.50
FAD	−2.12	0.38	−1.75	−1.75	−0.64	−0.82	0.30
FMN	−1.97	−1.35	−1.83	−1.86	−0.30	−0.70	0.42
FUC	0.17	−3.85	0.00	−0.20	−0.43	−0.07	−0.22
GAL	−0.75	−3.70	−1.30	−1.17	0.08	0.24	−0.16
GDP	−1.30	−1.30	−1.48	−1.34	−0.73	0.20	0.95
GLC	−1.31	−3.25	−1.35	−1.58	−0.40	−0.05	−0.03
HEC	−0.93	−0.47	−1.21	−1.48	−0.37	−1.31	0.29
HEM	−1.56	−0.73	−1.77	−1.92	−0.42	−1.43	0.64
MAN	−0.29	−3.93	−0.74	−0.78	−0.22	0.61	−0.01
MES	−0.01	−3.51	−0.86	−1.02	−0.49	0.52	−0.59
NAD	−1.71	−0.08	−1.75	−1.77	−0.23	−0.81	0.16
NAG	−0.24	−3.74	0.20	−0.05	0.03	0.31	−0.22
NAP	−1.79	−0.13	−1.51	−1.60	−0.33	−0.37	0.54
NDP	−1.93	0.03	−1.49	−1.38	−0.42	−0.55	0.57

The fingerprints correspond to the transformed properties (z-score) for the actual binding sites and are averaged for all of the proteins interacting with the same ligand.

Accuracy of localization estimated with the testing set

Best prediction

To objectively assess the accuracy of the method, we localized the binding sites for all proteins in the 20 data sets defined in Methods (Table 1). Accuracy varies significantly, depending on the type of binding site localized (Table 3). For ligands such as ATP, NAD, and FAD, there

Figure 5. Clustering of ligands according to their binding site fingerprints (Table 2). The distance between two ligands has been calculated as the Euclidean distance between their fingerprints and the tree was obtained with Phylip (J. Felsenstein, University of Washington, Seattle). Ligands that cluster together have similar binding sites. While ligands with the adenine moiety are close to each other, sugars are spread more broadly (Results).

is a clear difference between the accuracies of the predicted and random patches, indicating that the scoring function captures the salient features of these binding sites. For example, for the nicotinamide-adenine-dinucleotide (NAD), the accuracy of predicted patches (75%) is much higher than that of random patches (5%) (Fig. 7). In contrast, for ligands such as fucose, B-octylglucoside, and mannose, the accuracy of predicted patches is comparable to that of random patches.

Suboptimal solutions

The binding site may not correspond to the best scoring patch, but merely to a good scoring patch. In such cases, the optimizer may still find the binding site, although the correct prediction will not be top-ranked. To quantify this possibility, we calculated the average accuracy of the most accurate of the five and 10 best scoring patches, both for the optimized and random patches. Compared with considering only the best-scoring patch, accuracy increases slightly for the optimized patches (from 70% for the single top prediction to 80% and 84% for the most accurate among the top five and 10 scoring patches, respectively) and much more for random patches (from 3% to 21% and 42%).
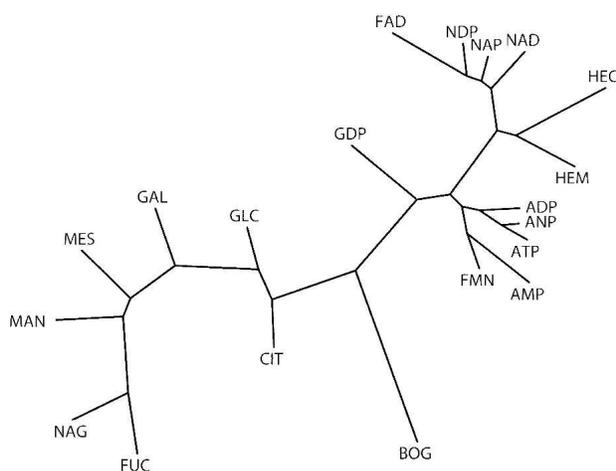
Accuracy as a function of the actual binding-site overlap cutoff

We investigated how the accuracy of localization is affected by the choice of the cutoff ϑ_0, which specifies the minimal degree of the predicted binding-site overlap with the actual binding site that is needed for a correct
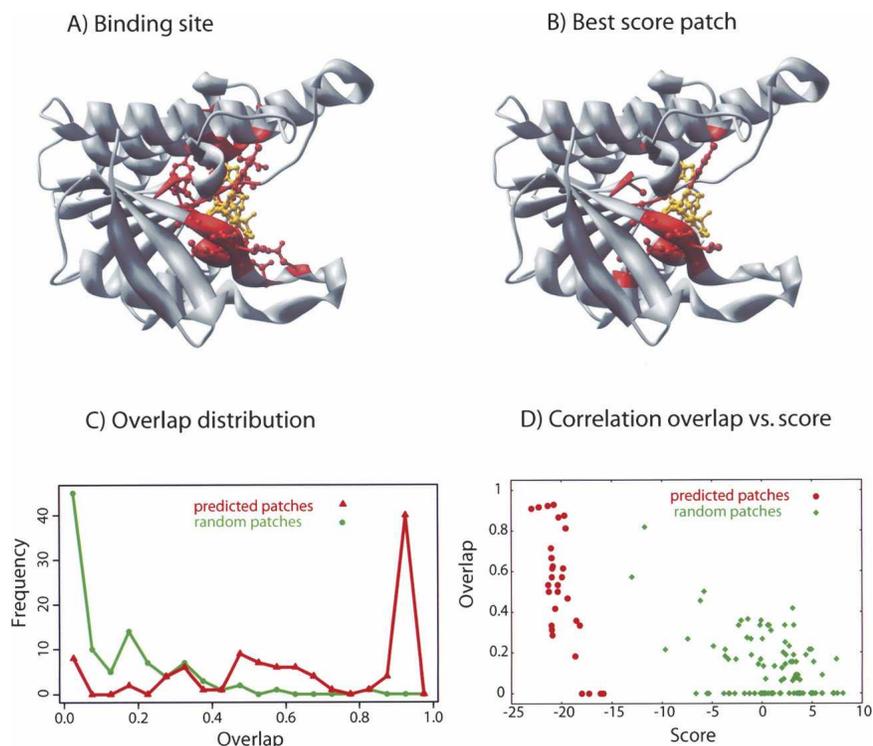
Figure 6. Detailed analysis of predictions for protein 1dhr. (*A,B*) In the *top* panels, the cofactor NAD is indicated in yellow, and the binding residues are in red. The actual location of the binding site (*A*) is very similar to the prediction (*B*). (*C*) Distribution of 100 optimized patches as a function of their overlap with the actual binding site. The distribution of the optimized patches (red curve) peaks at ~1 (maximum overlap), while random patches (green curve) peak at ~0 (no overlap). The optimizer is able to find the binding site, in most cases with an overlap larger than 0.5. (*D*) Scatter plot of the overlap vs. the score for the 100 optimized and random patches; the optimized patches have a lower score than random patches by construction (because of the optimization); moreover, they also have a higher overlap with the actual binding site.

prediction (see Methods). When the cutoff ϑ_0 is close to 1, only the best scoring patches that overlap completely with the known binding site will be counted as correct predictions. On the other hand, when ϑ_0 is close to 0, even patches that overlap only partially with the known binding site will be considered correct predictions. As expected, the accuracy of the method for every test set decreases as a function of the cutoff ϑ_0, both for the predicted binding sites and random patches (Fig. 7). For some ligands, almost all instances of their binding sites are correctly identified when the cutoff ϑ_0 is 0, which suggests that the best scoring patch is in the proximity of the known binding site rather than far away. In contrast, the poor performance for sugars is not affected by the choice of ϑ_0, indicating that the actual sugar binding-site locations are generally far from those of the best scoring predictions.

Discussion

We described, implemented, and benchmarked a method for integrating structure and sequence properties to pre-

dict the location of a binding site of specified type in a given protein structure. The method relies on a scoring function and a Monte Carlo optimization protocol to find a good scoring patch on the protein surface. The scoring function depends on z-scores of various properties of protein structure and sequence, including amino acid residue conservation, compactness, protrusion, convexity, rigidity, hydrophobicity, and charge density; the z-scores are calculated separately for each binding-site type from a set of previously characterized instances of the binding site on known protein structures (i.e., the training data set). We note that the binding site is not localized by the types of its residues, only by the degree of their conservation. Thus, we do not expect a strong dependence of localization on the degree of sequence similarity between the target sequence and the proteins in the training data set.

Combining information for localizing binding sites

Each of the previously described methods for localizing binding sites tends to rely on a relatively narrow set of

Table 3. *Accuracy for the 20 ligand types calculated for a single prediction (top_1) as well as for the most accurate prediction of the 5 (top_5) and 10 (top_10) best-scoring patches*

Ligand	top_1	Random	top_5	Random	top_10	Random
ADP	45.6	2.4	60.8	11.2	63.2	23.2
AMP	31.0	0.0	51.7	3.4	72.4	10.3
ANP	51.3	2.6	64.1	12.8	71.8	25.6
ATP	57.7	5.8	67.3	15.4	69.2	26.9
BOG	18.2	13.6	31.8	31.8	31.8	36.4
CIT	33.3	10.0	43.3	26.7	60.0	33.3
FAD	60.9	4.7	75.0	23.4	78.1	39.1
FMN	60.0	5.0	75.0	12.5	77.5	22.5
FUC	0.0	5.9	11.8	29.4	29.4	47.1
GAL	41.7	0.0	50.0	19.4	58.3	25.0
GDP	33.3	4.8	47.6	14.3	61.9	38.1
GLC	35.3	5.9	47.1	9.8	52.9	19.6
HEC	55.6	0.0	66.7	50.0	77.8	55.6
HEM	73.4	10.2	79.7	34.4	82.8	53.1
MAN	15.4	11.5	34.6	19.2	42.3	30.8
MES	29.4	2.9	47.1	14.7	55.9	20.6
NAD	55.6	5.1	73.7	21.2	75.8	39.4
NAG	4.5	4.5	15.2	19.7	22.7	31.8
NAP	65.4	3.8	69.2	23.1	76.9	26.9
NDP	58.3	0.0	66.7	16.7	70.8	41.7
Average	41.3	4.9	53.9	20.5	61.6	32.4
Maximum	73.4	13.6	79.7	50.0	82.8	55.6

For comparison, the accuracy is also calculated for random patches. The average accuracy for the single prediction is 41%. However, for some ligands (e.g., HEM, FAD, NAD, NAP, and NDP), the value ranges between 55% and 73%, while the random value is always <15%.

considerations. For example, docking methods consider geometrical complementarity and physical interactions (Kuntz et al. 1982); some methods search for cavities (Laskowski et al. 1996), and others look specifically at the residue types in the binding site or at their particular features (geometric hashing) (Artymiuk et al. 1994; Wallace et al. 1996, 1997; Kleywegt 1999; Oldfield 2002; Stark and Russell 2003; Stark et al. 2003). These methods vary in terms of the ligand and protein properties used, the search algorithm, and even the primary goal (i.e., the identification of the ligand type or the localization of the binding site). An advantage of our approach is the ability to integrate information from different sources into a single scoring function. At least in principle, consideration of more information should lead to more accurate predictions.

Localizing a binding site by patch optimization

To make integration straightforward, we chose a single representation of the system for all of the properties (see Methods). We represented the binding site as a patch of contiguous surface residues. Such patches have been used, for example, for the classification as well as prediction of protein–protein interactions by generating

a limited number of patches and assessing them according to a user-defined scoring function (Jones and Thornton 1997a,b).

The number of possible patches on the surface is generally too large for an exhaustive enumeration. For noncontiguous patches, the number of different patches of r residues on a protein with n surface residues is $\binom{n}{r} = \frac{n!}{r!(n-r)!}$ (e.g., $\sim 10^{22}$ for $r = 15$ and $n = 200$). The number of contiguous patches does not appear to be possible to estimate analytically, but it is still large enough to prevent an exhaustive enumeration. For this reason, we optimized a randomly created initial patch according to a scoring function rather than filter a manageable set of predefined patches by the scoring function. The advantages are that no manageable set of predefined patches needs to be constructed and that we are exploring the whole space of possible patches.

Performance of the optimizer

As in any optimization, our approach has two possible limitations: the optimizer and the scoring function. It is crucial to determine the power of the optimizer and the accuracy of the scoring function so that the future development effort is most productive. The role of the optimizer is to efficiently explore the space of all possible patches and find the best scoring one. For a given binding-site localization, when the optimization is carried out independently 100 times, starting with different random patches, the best-scoring solution is generally found in 30%–50% of the cases (e.g., Fig. 6). Because the initial random patches are generated independently, it is very likely that the most populated solution, which usually corresponds to the best-scoring solution, is the global minimum. Thus, the optimizer is not likely to limit the accuracy of the method, and future efforts on improving the method should focus on improving the scoring function.

Modularity of the method

Our scoring functions rely on a set of properties that are linearly combined using weights specific to each binding-site type. This modularity of the scoring function allows for flexibly modifying, adding, and removing properties without affecting the encoding of the other properties and the optimization protocol. Consequently, different scoring functions, including different weights, can be easily compared. Another difference from some of the previous methods (Jones and Thornton 1997a,b) is that the weights are not chosen by the user based on their experience, but are calculated for each binding-site type by relying on
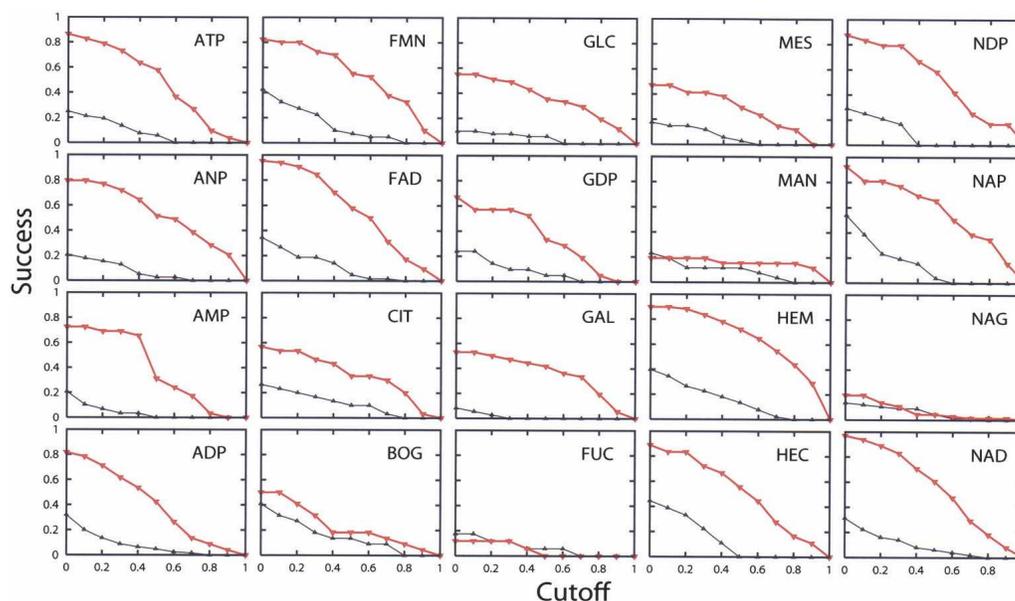
Figure 7. The accuracy of localization for the 20 ligand-binding sites as a function of the overlap cutoff ϑ_0, for both optimized patches (red curve) and random patches (black curve). As expected, for all ligands, the accuracy increases when ϑ_0 is decreased. The good localization of ligand binding sites for nucleotides, such as NAD, HEM, and NAP, contrasts with the poorer performance for sugars, such as GAL, MES, and FUC.

a set of known structures containing the corresponding binding site. Given the chemical and physical diversity of possible ligands, the ability to encode their binding sites by the importance of different properties is expected to be an advantage over methods that do not differentiate between different ligands (e.g., looking for the largest surface cavity). This expectation is clearly borne out by the different calculated property weights for the different ligand binding-site types.

Linear scoring function

We implemented and compared two different scoring functions, linear and quadratic, in the binding-site properties. While the linear model is widely used in general discrimination problems because of its simplicity, more sophisticated scoring functions may be able to better identify the actual binding site as the best scoring patch. One potential problem of the linear model is that the binding-site properties are not restrained to specific target values. The predicted patches may have property values that are larger or smaller than those of the real binding sites. For example, if known sample binding sites correspond to a cavity, the predictions will tend to be the largest cavities on the surface because those are most different from the mostly flat random patches; this rationale may not always work correctly, especially for smaller ligands. A similar concern applies to the charge density of a patch.

Quadratic scoring function

We also tested a second scoring function where the properties are restrained relative to their distributions in the sample binding sites. We use restraints quadratic in the properties and centered on the averages of the corresponding sample distributions. While the linear model has seven parameters, there are 13 in the quadratic scoring function (seven parameters for the centers of the distributions and six for the weights). By construction, the best-scoring patches tend to have property values close to those in the sample binding sites. However, the accuracy of localization relying on the quadratic function is generally not as high as in the case of the linear model; for example, for ADP it drops from 46% for the linear model to 26% for the quadratic model. Perhaps this is explained by the fact that the quadratic function depends only on the known positive examples of the localized binding-site type, while the linear model depends on the difference between the training examples and random patches.

The accuracy depends on the predicted ligand binding-site type

The benchmark shows that the accuracy of our method varies for different binding-site types (Fig. 7). In particular, the accuracy of localizing sugar-binding sites is poor. It is known that sugars display a variety of binding modes and that the protein–sugar interactions are difficult

to predict (Alberts et al. 2002). From a physical chemistry point of view, sugars interact with the protein through charged interactions that can be mediated by metal ions. From a biological point of view, sugars are used in a variety of biological processes. Such a variety of biological roles, which corresponds to a variety of binding modes, makes sugars a very difficult test set (del Sol Mesa et al. 2003). Incorporation of additional structural and sequence properties into the scoring function may result in improved localization.

Similar fingerprints produce similar localizations

We already showed that similar ligands have similar fingerprints (Fig. 5). We are now interested in whether similar fingerprints result in similar localization accuracies. If so, our localization method would be more useful for ligands with imprecisely determined fingerprints (i.e., ligands with few instances in the PDB). We localized five different ligands (i.e., ADP, FAD, FMN, HEM, and NAD) using their native fingerprints and the fingerprints for each one of the other four ligands. They all have similar fingerprints with high weights for conservation, protrusion, and convexity; HEM also depends strongly on hydrophobicity (Table 2). In general, using the native fingerprint results in the most accurate localization (data not shown). The non-native fingerprints reduce the accuracy of localization for 5%–15%. Considering that the localization accuracy ranges from 45% to 73%, fingerprints of similar ligands may therefore be used to localize binding sites for which only small training sets are available.

Toward the characterization of binding sites: Fingerprint specificity

Our current method has a precise and limited aim to localize the binding site for a given ligand type on a known protein structure. There are additional related problems, including predicting the type of the preferred ligand for a given binding site on a known structure. Properties that discriminate between binding sites and other regions of the protein, such as the seven properties used here, may also be effective in discriminating between different potential ligands for a given binding site. To find out how useful our fingerprints are for predicting the specificity of ligand binding, we performed the following experiment: For each of the 1008 structures in the 20 data sets, we assessed the scores of the 20 fingerprints applied to their native binding sites. Our fingerprints scored the native ligand best for 15.4% of the structures, which is three times better than the random rate (i.e., 1/20). Moreover, the success rate can only increase if we declare success when the native ligand is one of a few top-scoring ligands or when it is similar to the best-scoring ligand. Therefore, the fingerprints contain significant in-

formation about the specificity of the binding sites, although they are not sufficient on their own in their current form for a reliable identification of the ligand type.

We did not, however, address the most general question of predicting simultaneously both the location and type of the ligand binding sites on a given structure. A potential approach is to predict the best location for each available fingerprint, retain only the best scoring fingerprint for overlapping predicted locations, and finally apply a cutoff to the scores for the final prediction of both the location and type of the ligand-binding site. We do not expect that our current scoring function, developed for localization only, will be optimal for this integrated problem. For the current goal, the scoring function needs to maximize the difference between the tested binding site and a random patch. In contrast, for the prediction of the ligand type, the scoring function needs to maximize the difference between the alternative ligand types; thus, a different scoring function may be needed.

Some properties are more important than others

Because the localization problem was formulated as an optimization of a modular scoring function, it is relatively straightforward to further generalize the approach. For example, fingerprint weights for the conservation, protrusion, and concavity correlate with accuracy (Tables 2, 3). In contrast, fingerprint weights for compactness anti-correlate with accuracy (Tables 2, 3). Compactness is the only property that depends on the number of residues used to generate the patches and the only property designed specifically to restrain the shape of the patch rather than its location on the protein surface. Incorporating this feature via a linear term in the scoring function (i.e., the linear model) appears not to be the best solution.

We also analyzed how localization is affected by removing a property from the fingerprint. For ADP, for example, the properties with largest weights are conservation, protrusion, convexity, and compactness. The least-accurate localization is obtained when conservation is not used (30% vs. 46% for the full fingerprint), suggesting that conservation is the most important property in the ADP fingerprint. Localization accuracy also decreases without compactness (39%). Unexpectedly, localization accuracy slightly increases when protrusion and convexity are removed from the fingerprint (to 52% and 49%, respectively). This unexpected improvement might be a consequence of random error in the construction and assessment of fingerprints as well as of unaccounted correlations between the properties in the scoring function. Localization accuracy is essentially unaffected by removing rigidity (46%) and hydrophobicity (45%), while it slightly increases as a result of removing charge density (51%).

Improvement of the scoring function

We showed above that the method is not limited by the power of the optimizer; therefore, its accuracy must be limited by its scoring function. This accuracy might be increased as follows:

First, by optimizing the definitions of the current seven properties. For example, the Shannon entropy used here could be improved by considering the similarity between residue types instead of their identities.

Second, by adding new informative properties to the scoring function. For example, the proximity of the predicted patch to a PROSITE pattern may enhance the prediction for ligands such as ATP, because the P-loop motif is involved in the recognition of this ligand (Saraste et al. 1990).

Third, by improving the functional form of the scoring function. For example, cross-terms corresponding to the correlations between properties may be added.

Fourth, by optimizing the parameters of the scoring function based on the property distributions for random patches and known binding sites. For example, the weights could be determined by a Support Vector Machine (SVM) instead of the simple calculation used here (Vapnik 1995).

Fifth, as the PDB grows and is better annotated, the ligand binding-site fingerprints will be more accurate and can be more specific.

Applications

We tested our method for its ability to localize a given binding-site type on a target structure. It is conceivable that it can also be adapted to predicting the type of a ligand that binds to the structure in the first place. This might be achievable by constructing a comprehensive library of binding-site fingerprints, localizing each one of them on the structure, and predicting the putative ligands by considering the localized binding-site scores. Provided the library of fingerprints is sufficiently comprehensive, our approach could thus be applied to both the identification and localization of binding sites on hundreds of proteins determined by the structural genomics initiatives. Many of these structures correspond to sequences of unknown biological function (see introduction). When standard tools for protein sequence and structure comparison fail to find clear homologs, our approach may still be able to provide clues to the biological function of the protein.

In conclusion, we introduced an optimization-based approach for protein binding-site localization. In some of our tests, the method can correctly localize ~70% of the binding sites. A major advantage of the method is the integration of information from different sources, which is achieved through a ligand type–specific scoring function. The program is freely available at http://salilab.org/patcher. It is completely automated and can be applied to a large set of protein structures, such as those determined by the structural genomics projects and models predicted by large-scale comparative modeling (Burley et al. 1999; Brenner 2000, 2001; Sali 2001; Vitkup et al. 2001; Chance et al. 2002; Goldsmith-Fischman and Honig 2003).

Acknowledgments

References

Ahmad, S., Gromiha, M.M., and Sarai, A. 2004. Analysis and prediction of DNA-binding proteins and their binding residues based on composition, sequence and structural information. *Bioinformatics* **20:** 477–486.

Alberts, B., Johnson, A., Lewis, J., Raff, M., Roberts, K., and Walter, P. 2002. *Molecular biology of the cell*, 4th ed. Garland Science, New York.

Aloy, P., Querol, E., Aviles, F.X., and Sternberg, M.J. 2001. Automated structure-based prediction of functional sites in proteins: Applications to assessing the validity of inheriting protein function from homology in genome annotation and to protein docking. *J. Mol. Biol.* **311:** 395–408.

Armon, A., Graur, D., and Ben-Tal, N. 2001. ConSurf: An algorithmic tool for the identification of functional regions in proteins by surface mapping of phylogenetic information. *J. Mol. Biol.* **307:** 447–463.

Artymiuk, P.J., Poirrette, A.R., Grindley, H.M., Rice, D.W., and Willett, P. 1994. A graph-theoretic approach to the identification of three-dimensional patterns of amino acid side-chains in protein structures. *J. Mol. Biol.* **243:** 327–344.

Babbitt, P.C. 2003. Definitions of enzyme function for the structural genomics era. *Curr. Opin. Chem. Biol.* **7:** 230–237.

Bairoch, A. and Bucher, P. 1994. PROSITE: Recent developments. *Nucleic Acids Res.* **22:** 3583–3589.

Bork, P., Dandekar, T., Diaz-Lazcoz, Y., Eisenhaber, F., Huynen, M., and Yuan, Y. 1998. Predicting function: From genes to genomes and back. *J. Mol. Biol.* **283:** 707–725.

Brady Jr., G.P. and Stouten, P.F. 2000. Fast prediction and visualization of protein binding pockets with PASS. *J. Comput. Aided Mol. Des.* **14:** 383–401.

Brenner, S.E. 2000. Target selection for structural genomics. *Nat. Struct. Biol.* (Suppl.) **7:** 967–969.

———. 2001. A tour of structural genomics. *Nat. Rev. Genet.* **2:** 801–809.

Burley, S.K., Almo, S.C., Bonanno, J.B., Capel, M., Chance, M.R., Gaasterland, T., Lin, D., Sali, A., Studier, F.W., and Swaminathan, S. 1999. Structural genomics: Beyond the human genome project. *Nat. Genet.* **23:** 151–157.

Casari, G., Sander, C., and Valencia, A. 1995. A method to predict functional residues in proteins. *Nat. Struct. Biol.* **2:** 171–178.

Chakrabarti, P. and Janin, J. 2002. Dissecting protein-protein recognition sites. *Proteins* **47:** 334–343.

Chance, M.R., Bresnick, A.R., Burley, S.K., Jiang, J.S., Lima, C.D., Sali, A., Almo, S.C., Bonanno, J.B., Buglino, J.A., Boulton, S., et al. 2002. Structural genomics: A pipeline for providing structures for the biologist. *Protein Sci.* **11:** 723–738.

del Sol Mesa, A., Pazos, F., and Valencia, A. 2003. Automatic methods for predicting functionally important residues. *J. Mol. Biol.* **326:** 1289–1302.

Deremble, C. and Lavery, R. 2005. Macromolecular recognition. *Curr. Opin. Struct. Biol.* **15:** 171–175.

DeWeese-Scott, C. and Moult, J. 2004. Molecular modeling of protein function regions. *Proteins* **55:** 942–961.

Eisenstein, E., Gilliland, G.L., Herzberg, O., Moult, J., Orban, J., Poljak, R.J., Banerjei, L., Richardson, D., and Howard, A.J. 2000. Biological function made crystal clear—annotation of hypothetical proteins via structural genomics. *Curr. Opin. Biotechnol.* **11:** 25–30.

Elcock, A.H. 2001. Prediction of functionally important residues based solely on the computed energetics of protein structure. *J. Mol. Biol.* **312:** 885–896.

Fauchere, J. and Pliska, V. 1983. Hydrophobicity parameters pi of amino acids side chains from partitioning of N-acetyl-amino-acid amides. *Eur. J. Med. Chem.* **18:** 369–375.

Goldsmith-Fischman, S. and Honig, B. 2003. Structural genomics: Computational methods for structure analysis. *Protein Sci.* **12:** 1813–1821.

Goodford, P.J. 1985. A computational procedure for determining energetically favorable binding sites on biologically important macromolecules. *J. Med. Chem.* **28:** 849–857.

Greenbaum, D.C., Arnold, W.D., Lu, F., Hayrapetian, L., Baruch, A., Krumrine, J., Toba, S., Chehade, K., Bromme, D., Kuntz, I.D., et al. 2002. Small molecule affinity fingerprinting. A tool for enzyme family subclassification, target identification, and inhibitor design. *Chem. Biol.* **9:** 1085–1094.

Hardy, J.A. and Wells, J.A. 2004. Searching for new allosteric sites in enzymes. *Curr. Opin. Struct. Biol.* **14:** 706–715.

Jones, S. and Thornton, J.M. 1997a. Analysis of protein-protein interaction sites using surface patches. *J. Mol. Biol.* **272:** 121–132.

———. 1997b. Prediction of protein-protein interaction sites using patch analysis. *J. Mol. Biol.* **272:** 133–143.

Kinoshita, K. and Nakamura, H. 2003. Identification of protein biochemical functions by similarity search using the molecular surface database eF-site. *Protein Sci.* **12:** 1589–1595.

Kirkpatrick, S., Gelatt, C.D., and Vecchi, M.P. 1983. Optimization by simulated annealing. *Science* **220:** 671–680.

Kleywegt, G.J. 1999. Recognition of spatial motifs in protein structures. *J. Mol. Biol.* **285:** 1887–1897.

Kouranov, A., Xie, L., de la Cruz, J., Chen, L., Westbrook, J., Bourne, P.E., and Berman, H.M. 2006. The RCSB PDB information portal for structural genomics. *Nucleic Acids Res.* **34:** D302–D305.

Kuntz, I.D., Blaney, J.M., Oatley, S.J., Langridge, R., and Ferrin, T.E. 1982. A geometric approach to macromolecule-ligand interactions. *J. Mol. Biol.* **161:** 269–288.

Landgraf, R., Xenarios, I., and Eisenberg, D. 2001. Three-dimensional cluster analysis identifies interfaces and functional residue clusters in proteins. *J. Mol. Biol.* **307:** 1487–1502.

Laskowski, R.A., Luscombe, N.M., Swindells, M.B., and Thornton, J.M. 1996. Protein clefts in molecular recognition and function. *Protein Sci.* **5:** 2438–2452.

Laskowski, R.A., Watson, J.D., and Thornton, J.M. 2003. From protein structure to biochemical function? *J. Struct. Funct. Genomics* **4:** 167–177.

Liang, J., Edelsbrunner, H., and Woodward, C. 1998. Anatomy of protein pockets and cavities: Measurement of binding site geometry and implications for ligand design. *Protein Sci.* **7:** 1884–1897.

Lichtarge, O., Bourne, H.R., and Cohen, F.E. 1996. An evolutionary trace method defines binding surfaces common to protein families. *J. Mol. Biol.* **257:** 342–358.

Macchiarulo, A., Nobeli, I., and Thornton, J.M. 2004. Ligand selectivity and competition between enzymes in silico. *Nat. Biotechnol.* **22:** 1039–1045.

MacKerell, A.D., Bashford, D., Bellott, M., Dunbrack, R.L., Evanseck, J.D., Field, M.J., Fischer, S., Gao, J., Guo, H., Ha, S., et al. 1998. All-atom empirical potential for molecular modeling and dynamics studies of proteins. *J. Phys. Chem. B* **102:** 3586–3616.

Madabushi, S., Yao, H., Marsh, M., Kristensen, D.M., Philippi, A., Sowa, M.E., and Lichtarge, O. 2002. Structural clusters of evolutionary trace residues are statistically significant and common in proteins. *J. Mol. Biol.* **316:** 139–154.

Marti-Renom, M.A., Ilyin, V.A., and Sali, A. 2001. DBAli: A database of protein structure alignments. *Bioinformatics* **17:** 746–747.

Metropolis, N., Rosenbluth, A.W., Rosenbluth, M.N., Teller, A.H., and Teller, E. 1953. Equation of state calculations by fast computing machines. *J. Chem. Phys.* **21:** 1087–1092.

Miranker, A. and Karplus, M. 1991. Functionality maps of binding sites: A multiple copy simultaneous search method. *Proteins* **11:** 29–34.

Mirny, L.A. and Shakhnovich, E.I. 1999. Universally conserved positions in protein folds: Reading evolutionary signals about stability, folding kinetics and function. *J. Mol. Biol.* **291:** 177–196.

Moult, J. and Melamud, E. 2000. From fold to function. *Curr. Opin. Struct. Biol.* **10:** 384–389.

Neuvirth, H., Raz, R., and Schreiber, G. 2004. ProMate: A structure based prediction program to identify the location of protein-protein binding sites. *J. Mol. Biol.* **338:** 181–199.

Oldfield, T.J. 2002. Data mining the protein data bank: Residue interactions. *Proteins* **49:** 510–528.

Pawlowski, K. and Godzik, A. 2001. Surface map comparison: Studying function diversity of homologous proteins. *J. Mol. Biol.* **309:** 793–806.

Ringe, D. 1995. What makes a binding site a binding site? *Curr. Opin. Struct. Biol.* **5:** 825–829.

Rosen, M., Lin, S.L., Wolfson, H., and Nussinov, R. 1998. Molecular shape comparisons in searches for active sites and functional similarity. *Protein Eng.* **11:** 263–277.

Sali, A. 2001. Target practice. *Nat. Struct. Biol.* **8:** 482–484.

Saraste, M., Sibbald, P.R., and Wittinghofer, A. 1990. The P-loop—A common motif in ATP- and GTP-binding proteins. *Trends Biochem. Sci.* **15:** 430–434.

Schmitt, S., Kuhn, D., and Klebe, G. 2002. A new method to detect related function among proteins independent of sequence and fold homology. *J. Mol. Biol.* **323:** 387–406.

Shannon, C. 1948. A mathematical theory of communication. *Bell Syst. Tech. J.* **27:** 379–423, 623–656.

Silberstein, M., Dennis, S., Brown, L., Kortvelyesi, T., Clodfelter, K., and Vajda, S. 2003. Identification of substrate binding sites in enzymes by computational solvent mapping. *J. Mol. Biol.* **332:** 1095–1113.

Stark, A. and Russell, R.B. 2003. Annotation in three dimensions. PINTS: Patterns in non-homologous tertiary structures. *Nucleic Acids Res.* **31:** 3341–3344.

Stark, A., Sunyaev, S., and Russell, R.B. 2003. A model for statistical significance of local similarities in structure. *J. Mol. Biol.* **326:** 1307–1316.

Stuart, A.C., Ilyin, V.A., and Sali, A. 2002. LigBase: A database of families of aligned ligand binding sites in known protein sequences and structures. *Bioinformatics* **18:** 200–201.

Theodoridis, S. and Koutroumbas, K. 1999. *Pattern recognition.*. Academic Press, San Diego, CA.

Thornton, J.M., Todd, A.E., Milburn, D., Borkakoti, N., and Orengo, C.A. 2000. From structure to function: Approaches and limitations. *Nat. Struct. Biol.* (Suppl.) **7:** 991–994.

Vapnik, V.N. 1995. *The nature of statistical learning theory.* Springer-Verlag, New York.

Varughese, K.I., Skinner, M.M., Whiteley, J.M., Matthews, D.A., and Xuong, N.H. 1992. Crystal structure of rat liver dihydropteridine reductase. *Proc. Natl. Acad. Sci.* **89:** 6080–6084.

Vitkup, D., Melamud, E., Moult, J., and Sander, C. 2001. Completeness in structural genomics. *Nat. Struct. Biol.* **8:** 559–566.

Wallace, A.C., Laskowski, R.A., and Thornton, J.M. 1996. Derivation of 3D coordinate templates for searching structural databases: Application to Ser-His-Asp catalytic triads in the serine proteinases and lipases. *Protein Sci.* **5:** 1001–1013.

Wallace, A.C., Borkakoti, N., and Thornton, J.M. 1997. TESS: A geometric hashing algorithm for deriving 3D coordinate templates for searching structural databases. Application to enzyme active sites. *Protein Sci.* **6:** 2308–2323.

Wu, C.H., Apweiler, R., Bairoch, A., Natale, D.A., Barker, W.C., Boeckmann, B., Ferro, S., Gasteiger, E., Huang, H., Lopez, R., et al. 2006. The Universal Protein Resource (UniProt): An expanding universe of protein information. *Nucleic Acids Res.* **34:** D187–D191.

Yao, H., Kristensen, D.M., Mihalek, I., Sowa, M.E., Shaw, C., Kimmel, M., Kavraki, L., and Lichtarge, O. 2003. An accurate, sensitive, and scalable method to identify functional sites in protein structures. *J. Mol. Biol.* **326:** 255–261.

Zvelebil, M.J., Barton, G.J., Taylor, W.R., and Sternberg, M.J. 1987. Prediction of protein secondary structure and active sites using the alignment of homologous sequences. *J. Mol. Biol.* **195:** 957–961.